CURRENT RESEARCH ON SLOPE MOVEMENT IN MINES: USE OF HYPERSPECTRAL IMAGERY*

Edward L. McHugh,[1] Jami M. Girard,[1] Louis J. Denes,[2] Peter Metes,[2] and Charles Sabine[3]

[1]National Institute for Occupational Safety and Health, Spokane, WA; [2]Carnegie Mellon Research Institute, Pittsburgh, PA; [3]Geopix, Sparks, NV

ABSTRACT

The Spokane Research Laboratory, National Institute for Occupational Safety and Health, is investigating various remote sensing technologies as possible tools to detect, monitor, and mitigate hazardous situations in surface mines that could lead to catastrophic slope failure. Promising technologies include a field-portable spectro-polarimetric imager and a stationary interferometric radar device.

Field tests were conducted of a prototype visible and near-infrared spectro-polarimetric imager (SPI) built at the Carnegie Mellon Research Institute. The SPI employs an acousto-optical tunable filter (AOTF) to control wavelength, a phase retarder to measure polarization signatures, and a digital camera and computer to capture data. Images obtained at the Mountain Pass and Castle Mountain mines in southeastern California showed that the instrument is capable of obtaining hyperspectral images of highwalls, outcrops, hand samples and drill core in the field. We have retrieved spectra from Mountain Pass images that closely match those of bastnaesite and have had some success in classifying images. Although radio frequency noise in the data limited spectral classification of imagery, we project that careful alignment of the AOTF should minimize the noise and greatly improve classification.

INTRODUCTION

The Spokane Research Laboratory, National Institute for Occupational Safety and Health does mine safety and health research; a current project involves enhanced recognition of slope stability hazards at surface mines. Since 1995, 33 miners have died in slope failure accidents at surface mines in the US. A principal objective of the project is to improve the means for detecting conditions in open-pit mines that could lead to catastrophic slope failure. A contributing factor in many highwall failures is the presence and geometry of mechanically incompetent, clay-rich altered rock in pit walls. One element of the project is to test the application of imaging spectrometers to help recognize these weakened altered rocks. Most alteration minerals have diagnostic spectral absorption features in the short wave and mid-infrared that allow their identification by analysis of the light they reflect. Instruments are commercially available that can analyze light reflected from a single point, but an imaging system collects spectral reflectance data in a two-dimensional array. A secondary application of high-resolution imagery, beyond just identifying altered

Presented at the Fourteenth International Conference on Applied Geologic Remote Sensing, Las Vegas, NV, 6-8 November 2000.

rocks, would be to assist in compiling objective geologic maps of mine highwalls and other hazardous slopes from a safe position.

Although spectral imaging is the focus of this paper, a second area of remote sensing research for mine slope hazard detection is in the use of radar. High resolution radar imagery would complement spectral imagery for detailed remote geologic mapping in surface mines. Low-cost interferometric radar technology under development at Brigham Young University (BYU) shows promise for slope monitoring. Initial results of tests by BYU engineers for the Canadian National Railroad have demonstrated a capability for detecting rock falls and washouts along a right of way down to a few centimeters of displacement. Mine site tests of a stationary monitoring radar are planned.

INSTRUMENTATION

Field trials were conducted at MolyCorp's Mountain Pass Mine of a spectro-polarimetric imager (SPI) developed by Dr. Louis Denes at Carnegie Mellon Research Institute (Denes and others, 1998). The instrument is capable of obtaining multispectral images at visible and near-infrared wavelengths to generate a data cube that can be processed by standard hyperspectral techniques. The compact and field-portable instrument uses an acousto-optical tunable filter (AOTF) and an off-the-shelf, charge-coupled device (CCD) camera, offering great flexibility for quickly obtaining images in a variety of environments (Figure 1). The instrument was previously described by Gupta and others (1999) and Sabine and others (1999). Its demonstrated use in a field environment could lead to development of ground-based imagers in different spectral ranges, e.g., 1000 to 2500 nanometers (nm), that would help to distinguish and map other mineral materials including clay-rich altered zones (see Clark and others, 1993).

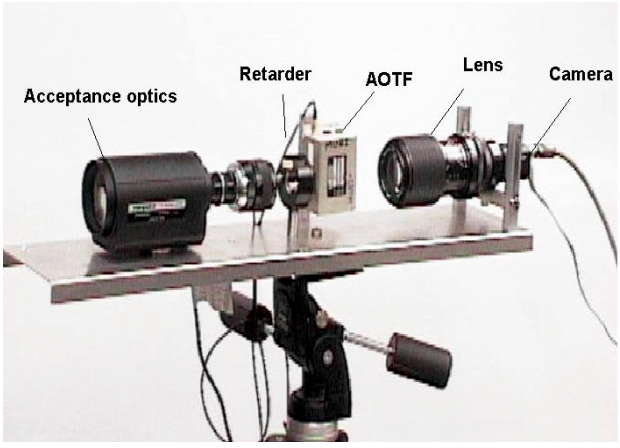

Figure 1. Spectro-polarimetric imager components.

Established hyperspectral imaging systems, such as AVIRIS and HYDICE, are based on conventional diffraction gratings and prisms with two-dimensional detector arrays (Porter and Enmark, 1987; Rickard and others, 1993). Such systems operate in either whiskbroom or pushbroom mode and collect data in hundreds of narrow spatial bands to build an image. Designed for airborne applications, they are generally heavy and bulky. The AOTF-based imaging system samples an entire two-dimensional scene at once with no moving parts, making it compact and robust. The programmable AOTF allows rapid sequential or random tuning for different spectral bands over a wide wavelength range.

The spectro-polarimetric imager consists of a tellurium dioxide (TeO_2) AOTF crystal, radio frequency (RF) electronics, image-forming optics, a charge-coupled device (CCD) camera, and an external host computer with a frame grabber board and control and processing software. A summary of the imager specifications are listed in table 1. During operation of the AOTF, an RF acoustic wave is applied to a birefringent TeO_2 crystal through an attached piezoelectric transducer. This traveling acoustic wave sets up a diffraction grating so that light incident on the crystal produces a diffracted beam with a shift corresponding to wavelength resulting from the phase-matching condition. The wavelength of the diffracted light is selected

by tuning the applied RF frequency. The center wavelength of the optical passband in the AOTF is inversely proportional to the applied RF and can be programmed in the host computer for very rapid selection of desired spectral and polarization parameters.

Table 1. Specifications

Parameter	Value
Spectral range	450-1000 nm
Resolution	10 @ 600 nm
Switching rate	30 microsec/band
Retarder range	400-1800 nm
AOTF aperture	15×15 mm
Rf range	25-60 MHz
Rf power	<1 W
Field of view (adjustable)	1.6 to 16 Deg

Light entering the instrument first passes through the acceptance optics, which collimate the light before it passes through a phase retarder and the AOTF. Active zoom control on the acceptance optics provide a field of view adjustable from 1.6˚ to 16˚. The liquid crystal variable phase retarder provides optional polarimetric control for the imaging system. Varying the voltage applied to the retarder controls the amount of phase delay between the components, changing the polarization state of the incoming light. The AOTF acts as an analyzer by transmitting only vertically polarized light. For natural scenes in the visible spectrum, polarized light is primarily horizontal in orientation. By varying retardation, polarization signatures of points in the scene including the polarization angle and magnitude are transmitted to the CCD camera.

Software in the host computer sets the spectral range, spectral bandwidth, and polarization parameters for data collection. Two control modes can be used at 30 microseconds per spectral band over wavelengths of 450 to 1000 nm. In sweep mode, the AOTF sequences through the full spectral range of the instrument, collecting the maximum amount of information in a scene. In switching mode, the instrument alternates between a small number of parameter settings for quick collection of specific bands for the sampled scene. The switching mode can be programmed to obtain real-time band ratio images.

MOUNTAIN PASS DATA

The Mountain Pass Mine, which lies about 60 miles southwest of Las Vegas, Nevada, was selected because the diagnostic spectral features of its rare-earth mineral assemblage are in the spectral range of the present instrument. Data were collected at the mine in July 1999. Images were also collected at the nearby Castle Mountain gold mine, operated by Viceroy Gold Corp., for comparison of images, spectra, and methodology. Additional images were collected in the Carnegie Mellon laboratory in December 1999 and June 2000. These images of hand specimens under artificial light sources were used as an aid in calibration and evaluation of the instrument. Thin sections were made of both ore and host rocks to assist in interpreting spectral images.

The Mountain Pass deposits occur as carbonatite veins associated with potassium-rich igneous rocks that intrude a block of Precambrian metamorphic rocks. The carbonatites, apparently of magmatic origin, consist mainly of calcite, dolomite, ankerite, and siderite. Bastnaesite, a fluorocarbonate of lanthanide series metals and the principle rare-earth bearing mineral present, constitutes 5 to 15 percent of much of the orebody and locally exceeds 60 percent (Olson and others, 1954). Rare-earth elements of the lanthanide series (cerium, lanthanum, neodymium, europium and others) produced at the Mountain Pass Mine are used in petroleum and pollution control catalysts, specialty glasses and magnets, and television and computer

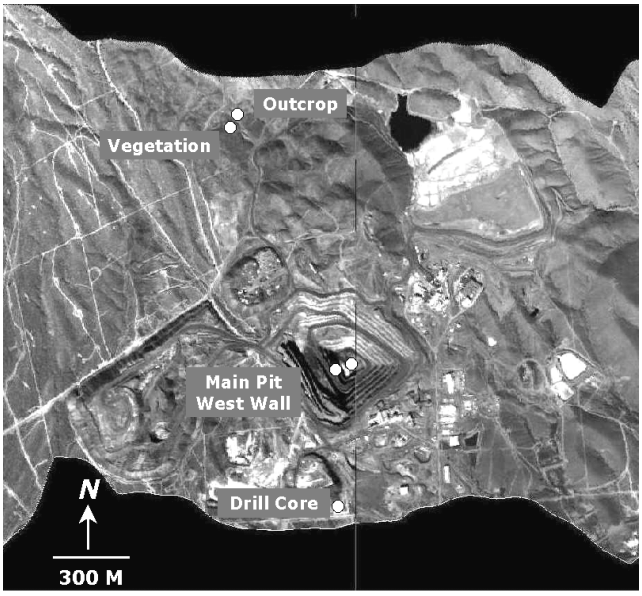

Figure 2. Low-level AVIRIS scene (October 1999) showing ground-based image collection sites.

monitor phosphors. Diagnostic spectral characteristics of the rare-earth assemblage correspond to published spectra of neodymium oxide, with at least eight distinctive absorption features between 450 and 1000 nm. Spectral reflectance data for the deposit were published by Rowan and others (1986); work with AVIRIS data for the deposit was described by Kingston (1993) and Rowan and others (1996).

Twelve multispectral images, including pit highwalls, outcrops, drill core from the ore zone, and hand samples, were collected at the Mountain Pass Mine. Collection sites are shown in Figure 2; example images are in Figure 3. The data consist of 47 bands from 480 to 940 nm in 10 nm intervals each collected at four polarizations. For each scene, original raw data comprising 190 bitmap files were compiled into data cubes using ENVI software. The default 2% stretch was turned off before compilation and some files were spatially subset to reduce registration errors caused by wind-induced camera shake during data collection.

Original data sets consisted of 640x480 pixel images; the images were cropped to eliminate dark margins in some scenes. Each analyzed scene contained white and black cards that were used for data correction and normalization. Mean values from a region of interest in the black card were used to correct for path radiance using ENVI's dark subtraction routine. A region of interest in the white card was used to normalize the data to relative reflectance using ENVI's flat field calibration technique.

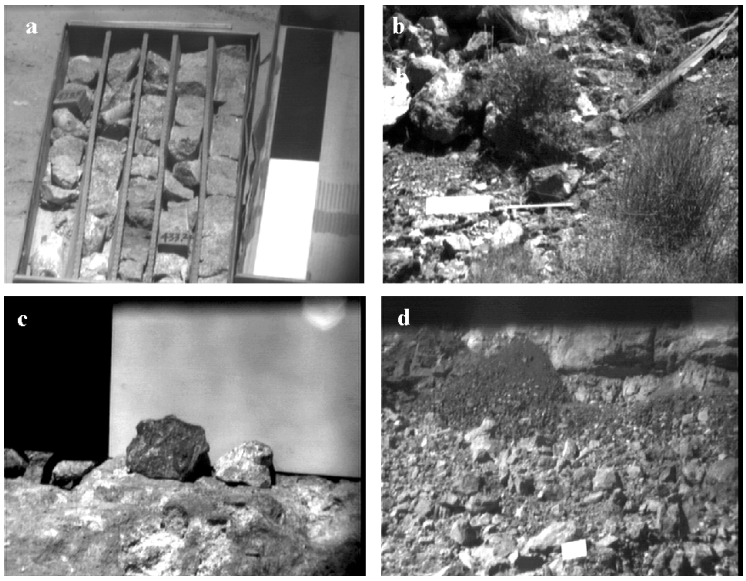

Figure 3. SPI images showing (a) drill core; (b) vegetation and outcrop; (c) hand samples; and (d) wall in main pit.

Reflectance spectra of Mountain Pass rare-earth ore were measured for this study with an ASD full-range spectrometer at 1-nm resolution and resampled to 10-nm resolution. These profiles had very good agreement with U.S. Geological Survey library profiles for neodymium oxide (Clark and others, 1993) and were used to evaluate the SPI images. The most useful prominent features occur at approximately 740 nm, 800 nm, and 870 nm.

Data were compiled into image cubes and basic analysis was done for each of the scenes, but this paper focuses on images from the west highwall of the main pit at Mountain Pass. The area of the highwall

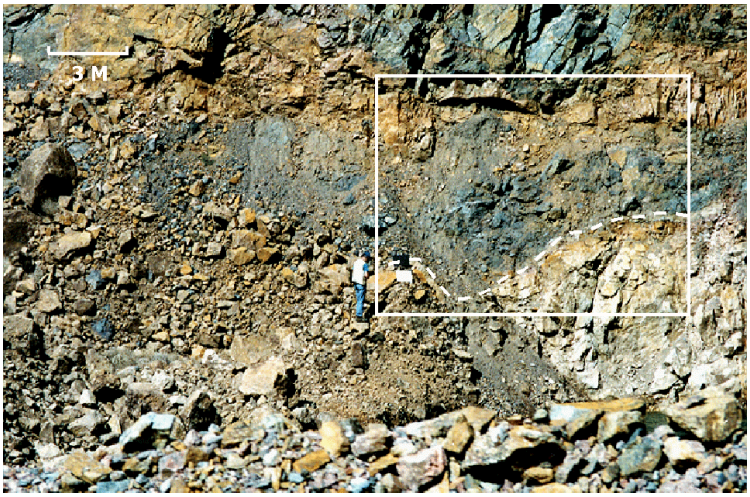

Figure 4. West wall of the Mountain Pass Mine main pit, showing the area of the spectral image in figure 5.

included in this data set is shown in Figures 4 and 5; the dashed line shows the approximate contact of the ore zone (lower portion) with host rocks (upper portion).

Original images (640x480 pixels, see Figure 5) were cropped at the top, left, and right sides, resulting in a 622x388 pixel, 47-band data cube. Plane-polarized images showed minor registration errors from camera shake during data acquisition, and elevated random noise at the high and low ends of the spectral range. A second artifact in the images is a set of near-vertical to diagonal light and dark stripes resulting from RF noise at the AOTF crystal/transducer boundary, due in part to misalignment caused by accidental jarring during transport. ENVI band math scripts generated an averaged image set by combining all four polarization images into a single data cube. Although some spatial resolution was lost in the averaged data, the combined images showed significant improvement in random noise distribution. Resulting spectral profiles were also smoothed in the combination. Only minor improvement was shown in the RF striping noise component. The discussion that follows relates to the combined polarization image set. Dark subtraction was done with a 276-pixel black card region of interest, and normalization to relative reflectance was done with a 231-pixel white card region of interest.

A sampling of single pixels from the resulting data cube showed numerous spectral profiles that are related to the expected rare-earth mineral assemblage. SPI spectra in Figure 6, offset 4 percent of full scale for clarity, show a range of correlation with the spectra measured from Mountain Pass bastnaesite ore with the ASD spectrometer. Some of the profiles match nearly all the characteristic absorption features for the ore (e.g., pixel x:108, y:77); several show the asymmetry at the 790-800-nm feature.

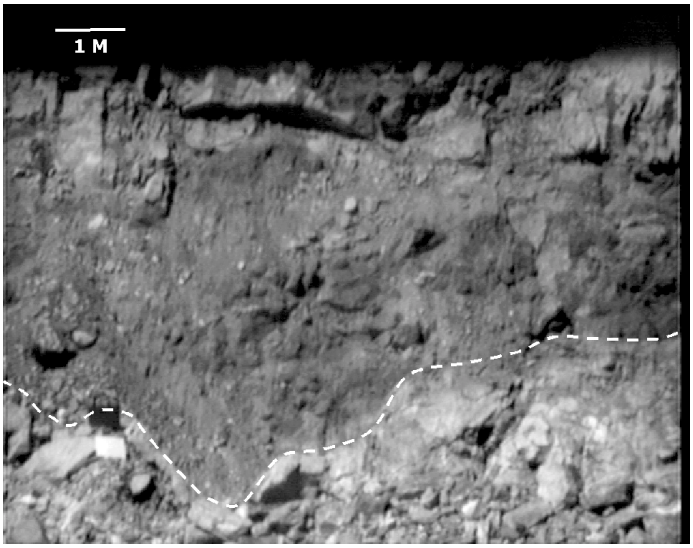

Figure 5. Original polarized image at 600 nm and 0˚ polarization.

IMAGE CLASSIFICATION

A first classification of the normalized images, using ENVI's Spectral Angle Mapper (SAM) at the default spectral angle (0.10 radians), was based on two end members defined as regions of interest (roi) for presumed "ore" and "host" portions of the image. The result was quite reasonable and the size of the roi polygons had little effect on the outcome. Roi ranging from 60 to more than 2500 pixels

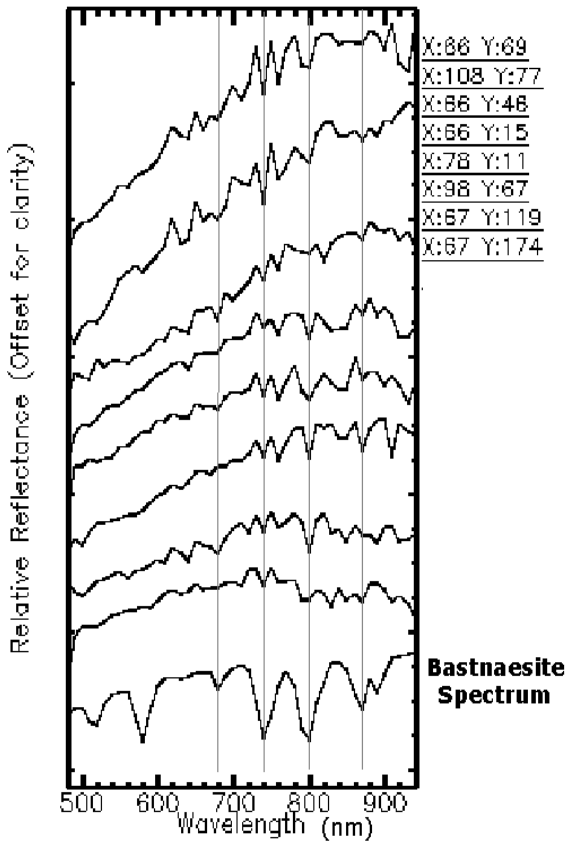

Figure 6. Sampling of spectra from the main pit west wall that correlate with bastnaesite.

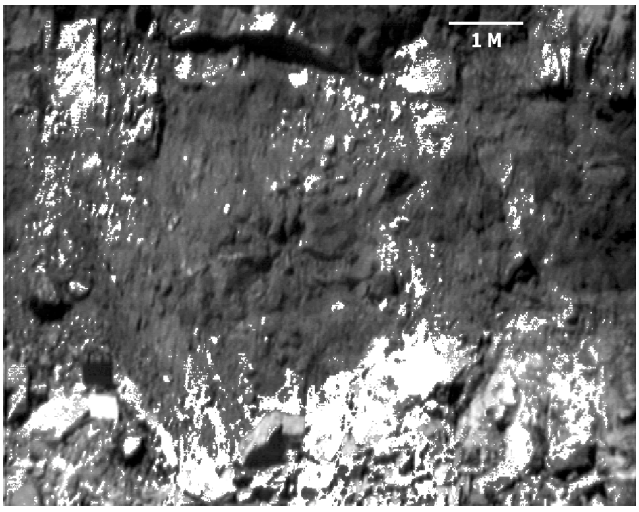

Figure 7. SAM classification on the west wall image following a cross-track illumination correction; white areas classified as ore.

returned approximately the same result leaving about 20% of the image unclassified. A cross-track illumination correction (multiplicative, two polynomials) was applied to the original images to reduce the effect of RF striping from the AOTF. The correction reduced near-vertical striping and an apparent x-axis gradient in the original images. SAM classification of the result included larger areas of ore end-member correlation in the left side of the image, areas that were left unclassified without the cross-track correction (Figure 7). The lower portion of the image is predominantly ore; the patchy isolated classified polygons in near-vertical stripes are likely associated with RF noise.

A second strategy applied similar classification methods to the west wall image after applying ENVI's Minimum Noise Fraction (MNF) transformation, using eight to eleven transformed bands. The transformation was useful for reducing random noise but was generally unsuccessful in reducing the RF striping. Several supervised classification methods and settings with the transformed images showed no particular improvement over that shown in Figure 7.

ENVI's Pixel Purity Index™ function applied to the MNF transformed data (1200 iterations and a threshold factor of 3) highlighted an endmember with a profile that closely matched most of the neodymium peaks in position and amplitude. However, classifications based on this endmember profile identified only very small areas within the scene. Profiles for other apparent endmembers had no features that relate to rare earths.

A third strategy for distinguishing ore-bearing parts of the image made use of ENVI's matched filtering routines for partial unmixing to find a predetermined endmember. The resampled ASD spectral profile for bastnaesite ore was used as the known endmember. The resulting classification, shown in Figure 8, was relatively successful in identifying ore in the lower portion of the image. Again, vertical striping in the image relates to the RF noise.

CONCLUSIONS

The field tests were designed to evaluate the use of high resolution imagery to remotely characterize the mineral composition of pit slopes. The SPI visible/near infrared images clearly illustrate the capabilities of the method to collect a multispectral image and discriminate materials within the image, validating the concept of simplified spectral imaging for such purposes. To apply the AOTF-based technology to more common geologic materials, the instrument needs to extend further into the infrared. Images in the 2 to 2.5 micrometer part of the infrared spectrum, where spectral features for clays are more distinctive, would be more useful for mapping altered zones in a highwall.

The field test data allowed isolation of spectral profiles that correlate with rare-earth elements expected at the site. However, the signal-to-noise ratio in the data limited detailed classification of the images; spectral features within the profiles may be broader and shifted from standard library positions. A next-generation instrument will improve the signal-to-noise ratio and optimize calibration for more reliable profile matching. Additional work needs to be done on making use of the polarization content of the AOTF images.

Figure 8. Matched filtering classification, white areas correspond to bastnaesite spectrum.

Where detection and recognition may require only a limited set of specific spectral bands, depending on the material sampled and backgrounds, an AOTF allows high-speed spectral selectivity with high resolution. Such capability greatly reduces the amount of data collection and processing required. The instrument can be used in the field with minimal maintenance or special handling; its demonstrated use is a first step in development of imagers for a wide range of geologic materials.

REFERENCES

R. N. Clark, G. A. Swayze, A. J. Gallagher, T. V. V. King, and W. M. Calvin, 1993, "The U. S. Geological Survey, Digital Spectral Library: Version 1: 0.2 to 3.0 microns," *U.S. Geological Survey Open File Report* 93-592, 1340 pages, http://speclab.cr.usgs.gov.

L. J. Denes, M. Gottlieb, and B. Kaminsky, "Acousto-Optic Tunable Filters in Imaging Applications," *Opt. Eng*. 37, pp. 1262–1267, 1998.

N. Gupta, R. Dahmani, M. Gottlieb, L. Denes, B. Kaminsky, and P. Metes, "Hyperspectral Imaging Using Acousto-Optical Tunable Filters." In *Proceedings of SPIE*, v. 3718, 10 pp. 7-9 April 1999.

M. J. Kingston, "Evaluation of AVIRIS Data for Mineral Mapping at Mountain Pass, the East Mohave Desert, California." In *Proceedings of the Ninth Thematic Conference on Geologic Remote Sensing*, Pasadena, CA, pp. 181-182, 8-11 February 1993.

J. C. Olson, D. R. Shawe, L. C. Pray, and W. N. Sharp, 1954, "Rare-earth Mineral Deposits of the Mountain Pass District, San Bernardino County, California," *U.S. Geological Survey Prof. Paper* 261, 75 p.

W. M. Porter, and H. T. Enmark, "A System Overview of the Airborne Visible/Infrared Imaging Spectrometer," *JPL Publication* 87-38, pp. 3–12, 1987.

L. J. Rickard, R. Basedow, E. Zalewske, P. R. Silverglate, and M. Landers, "HYDICE: an airborne system for hyperspectral imaging." In *Proceedings of SPIE*, v. 1937, pp. 173–179, 1993.

L. C. Rowan, R. N. Clark, and R. O. Green, "Mapping Minerals in the Mountain Pass, California Area using the Airborne Visible/Infrared Imaging Spectrometer (AVIRIS)." In *Proceedings of the Eleventh Thematic Conference and Workshops on Applied Geologic Remote Sensing*, Las Vegas, NV, pp. 175-176, 27-29 February 1996.

L. C. Rowan, M. J. Kingston, and J. K. Crowley, "Spectral Reflectance of Carbonatites and Related Alkalic Igneous Rocks: Selected Sampled from Four North American Localities," *Economic Geology*, v. 81, pp. 857-871, 1986.

Charles Sabine, L. J. Denes, M. Gottlieb, B. Kaminsky, P. Metes, R. T. Mayerle, and J. M. Girard, "A Portable Spectro-Polarimetric Imager: Potential Mine Safety and Geologic Applications." In *Proceedings of the Thirteenth International Conference on Applied Geologic Remote Sensing*, v. I, Vancouver, Canada, pp. I-190-194, 1-3 March 1999.